International Journal of Nanomedicine

Dovepress
open access to scientific and medical research

Open Access Full Text Article

ORIGINAL RESEARCH

Plasma SiOx:H Nanocoatings to Enhance the Antibacterial and Anti-Inflammatory Properties of Biomaterials

Ye Han[1], Qingsong Yu[2], Xiaoqing Dong[3], Jianxia Hou[1,*], Jianmin Han[4,*]

[1]Department of Periodontology, Peking University School and Hospital of Stomatology & National Center of Stomatology & National Clinical Research Center for Oral Diseases & National Engineering Laboratory for Digital and Material Technology of Stomatology & Beijing Key Laboratory of Digital Stomatology & Research Center of Engineering and Technology for Computerized Dentistry Ministry of Health & NMPA Key Laboratory for Dental Materials, Beijing, People's Republic of China; [2]Department of Mechanical and Aerospace Engineering, University of Missouri, Columbia, MO, USA; [3]Marketing Department, PlasmaDent Inc., Columbia, MO, USA; [4]Department of Dental Materials, Peking University School and Hospital of Stomatology & National Center of Stomatology & National Clinical Research Center for Oral Diseases & National Engineering Laboratory for Digital and Material Technology of Stomatology & Beijing Key Laboratory of Digital Stomatology & Research Center of Engineering and Technology for Computerized Dentistry Ministry of Health & NMPA Key Laboratory for Dental Materials, Beijing, People's Republic of China

*These authors contributed equally to this work

Correspondence: Jianmin Han; Jianxia Hou, Tel +86-10-82195746; +86-13683696349, Fax +86-10-62164691; +86-10-82195496, Email hanjianmin@bjmu.edu.cn; jxhou@163.com

Purpose: To evaluate the antibacterial and anti-inflammatory properties of SiOx:H nanocoatings using a plasma-deposition technique.
Materials and Methods: Four groups of SiOx:H nanocoatings were prepared by plasma nanocoating technique using different deposition gases and durations, specifically trimethylsilane (TMS) for groups A1 and A2 and a mixture of TMS and oxygen for groups B1 and B2. Changes in surface chemistry and physical properties were measured. *Staphylococcus aureus* and *Streptococcus mutans* were cultured on plasma SiOx:H nanocoatings to evaluate antibacterial and antibiofilm formation activities. Human gingival fibroblasts (HGFs) and HaCaT human keratinocytes were cultured and stimulated with tumor necrosis factor-α (TNF-α). Cell viability was measured using a Cell Counting Kit-8 (CCK-8) assay. Quantitative real-time polymerase chain reaction (qRT-PCR) and enzyme-linked immunosorbent assay (ELISA) were used to evaluate anti-inflammatory properties, including the mRNA and protein levels of inflammatory mediators and proinflammatory cytokines.
Results: The carbon content was dominant in group A nanocoatings and the oxygen and silicon elements were dominant in group B nanocoatings. Groups A2 and B2 were approximately threefold thicker than groups A1 and B1. The plasma SiO_x:H nanocoatings decreased bacterial growth and biofilm formation by 30–70% ($p < 0.05$). Scanning electron microscopy (SEM) revealed damaged biofilm structures. Moreover, the antibacterial properties of group B were greater than group A, and the antibacterial properties of groups A2 and B2 were more effective than A1 and B1, respectively. CCK-8 assays revealed the plasma SiOx:H nanocoatings had good biocompatibility. Furthermore, under TNF-α-induced inflammation, the mRNA and protein levels of interleukin-6, interleukin-8, cyclooxygenase-2, and monocyte chemoattractant protein-1 were downregulated in the plasma SiOx:H nanocoating groups ($p < 0.05$).
Conclusion: Plasma SiOx:H nanocoatings exerted antibacterial and anti-inflammatory effects with excellent biocompatibility. Therefore, the plasma SiOx:H nanocoating technique has potential for implant materials and other medical devices.
Keywords: plasma SiOx:H nanocoating technique, biomaterial-related infection, bacterial adhesion, biofilm formation, anti-inflammation

Introduction

In dentistry, clear aligners must be worn for 20–22 h daily, whereas dental implants last a lifetime. Both types of devices are ideal substrates for bacterial adhesion and biofilm formation, inducing sustained inflammatory processes and failure of biomedical devices.[1] Bacteria attach to biomaterial surfaces and form biofilm.[2] Pathogenic biofilms are involved in ≥65% of nosocomial infections.[3] A mature biofilm is more difficult to eliminate than planktonic bacteria. Furthermore,

Received: 20 September 2021
Accepted: 15 January 2022
Published: 28 January 2022

bacteria in biofilms activate innate and adaptive host defenses, triggering immuno-inflammatory responses. Upon bacterial invasion, inflammatory mediators are secreted, including cytokines that attract leukocytes and neutrophils, inducing inflammation.[4] In addition, host cells produce reactive oxygen species, cytokines, and other small molecules that amplify and sustain the inflammatory response, while causing progressive tissue destruction.[5]

Biomaterial-associated infections usually require difficult and expensive treatments. Infections can be prevented by surface modification of biomaterials with antibiotics and other agents, but such modified surfaces tend to degrade.[6] Nanomaterials coated by various physical and chemical methods with functional groups, such as metal/metal oxide nanoparticles, have been successfully applied to improve the anti-bacteria and biological effects. The controllable metal ions release of metal/metal oxide nanoparticles presents an opportunity to eliminate resistance and surges of bacteria, and to enhance their antibacterial activities leading to potential clinical applications.[7] Metal nanoparticles, such as AuNPs and Cu2O, showed good inhibitory effects against bacteria and fungi.[8–10] Ag nanospheres with sustained and controllable release of Ag ions exhibited significant antibacterial ability and also showed good cytocompatibility.[11] A review article reported that gold nanoclusters are promising antimicrobial agents due to their high biocompatibility, ease of modification, and photothermal stability.[12] In addition, attempts have been made to improve biological properties, including biocompatibility and osteogenic activity, by methods such as coating poly-L-lactic acid scaffolds coated with Zn-doped mesoporous silica.[13] Recent studies have been focusing on improving the anti-inflammatory properties of biomaterials. Biomimetic chitosan-based scaffolds have been reported to improve bone tissue regeneration and control the inflammatory responses.[14] Visalakshan used a plasma polymerization technique to create a nanothin model of biomaterial coatings and achieved a desirable innate immune response.[15]

Plasma nanocoating is a new technology for biomaterial surface modification and is controllable and stable Plasma nanocoating produces stable biomaterial surfaces by covalent bonding to the substrate.[16] Surface modification can be readily achieved by controlling the plasma gas composition, system pressure, gas flow rate, and deposition time. Plasma-derived coatings can be deposited on practically any type of substrate material.[15] Plasma coatings deposited using oxygen, argon, or nitrogen are applied to dental materials to facilitate osseointegration, inhibit bacterial attachment, and reduce inflammation.[17] Recently, plasma coating with non-stoichiometric silicon oxides (SiOx) have been widely used for biomaterial surface modification. Plasma SiOx:H nanocoating using trimethylsilane (TMS) and O2 at different molar ratios could yield well-controlled surface chemistry and wettability by controlling the plasma gas compositions.[18] Plasma SiOx:H nanocoatings exhibit stable chemical and mechanical properties in electronics applications.[16] In addition, plasma SiOx:H nanocoatings have good biocompatibility[19] and accelerate re-endothelialization.[20]

Nanoscale plasma coating of TMS and oxygen on the surfaces of silicone rubber can inhibit the formation of *Staphylococcus aureus* (*S. aureus*) biofilm. The mechanism may involve altered surface protein adsorption caused by changes in surface chemistry, including albumin, fibrinogen, and fibronectin.[21] However, few studies have evaluated the antibacterial effects of SiOx:H nanocoating using different plasma deposition conditions. The most common oral pathogen, *Streptococcus mutans* (*S. mutans*), can adhere to teeth or dental biomaterials.[6] Here, we evaluated the antibacterial properties of plasma SiOx:H nanocoatings using *S. mutans* and *S. aureus*. Furthermore, the biological effects of plasma coatings, including SiOx:H nanocoatings, on inflammatory cells are unclear. Few studies have explored whether plasma coatings enhance antibacterial activity and biocompatibility simultaneously, which are associated with the long-term success of biomaterials. However, the antibacterial activity and biocompatibility, especially anti-inflammatory properties, are sometimes contradictory because cytotoxicity is often associated with the antibacterial activity.[21] The key requirements of surface modification are to achieve good biocompatibility, while inhibiting bacteria, to balance the race between bacteria and cells. Therefore, we investigated the antibacterial and anti-inflammatory properties of plasma SiOx:H nanocoatings simultaneously.

Materials and Methods

Plasma Nanocoating Preparation

Zendura FLX dental aligner membranes of dimensions 0.76×125 mm (thickness × diameter) were purchased from Bay Materials (Fremont, CA, USA). Argon gas (purity >99.999%) and oxygen gas (purity >99.6%) were purchased from Airgas (Columbia, MO, USA). TMS (purity >97%) was purchased from Gelest, Inc. (Morrisville, PA, USA).

An 80 L bell jar-type plasma reactor was used to deposit plasma nanocoatings on Zendura FLX dental aligner membrane surfaces. Plasma discharge was initiated and sustained using a 13.56 MHz RF power supply (RFX-600; Advanced Energy Industries, Inc. Fort Collins, CO, USA). Before introducing plasma gases, the plasma reactor was first evacuated to a base pressure of 1 mTorr using a pump group consisting of mechanical and booster pumps connected in series. The flow rate of plasma gases was controlled using MKS mass flow controllers (MKS Instruments, Andover, MA, USA) and an MKS Model 247C readout. The pressure inside the plasma reactor was stabilized and sustained using an MKS pressure controller.

Prior to plasma coating, the dental aligner membrane surfaces were first cleaned by pretreatment with argon plasma for 5 min at a 1 sccm argon flow rate, 50 mTorr pressure, and 20W RF power. Next, plasma nanocoatings were deposited using trimethylsilane (TMS) or a mixture of TMS and oxygen at a 50 mTorr pressure and 30W RF power. Dental aligner membranes plasma-nanocoated using TMS plasma were designated as groups A1 and A2, which had coatings of different thicknesses. Plasma-nanocoated using a mixture of TMS and O_2 were designated as group B1 and B2, which had coatings of different thicknesses. During plasma coating process, Si wafers (1cm×1cm) were attached to the dental aligner surfaces to monitor the nanocoating thickness of plasma SiOx:H nanocoatings.

Surface Characterization

The thickness of plasma SiOx:H nanocoatings was determined using a Filmetrics F40 microscope thin-film analyzer. The surface wettabilities of plasma-nanocoated and uncoated dental aligner membranes were assessed based on water contact angle measurements using a Contact Angle Meter/Goniometer (DMe 210; Kyowa Interface Science Co., Ltd., Eden Prairie, MN, USA) with FAMAS software. At least six measurements were obtained per condition and used to determine the mean contact angle and standard deviation. Membrane composition was evaluated using an X-ray photoelectron spectrometer (XPS; Kratos Analytical Inc., Chestnut Ridge, NY, USA). Data were analyzed using Casa XPS software. The surface morphologies and roughness of different plasma SiOx:H nanocoatings were examined by atomic force microscopy (AFM; PI3800/SPA400, Seiko Instruments, Japan) and five fields were randomly selected from each sample for analysis. Bovine serum albumin (BSA) at a concentration of phosphate-buffered saline (PBS) was used for protein adsorption assay. Aliquots of 200 uL were deposited onto the nanocoated membranes in 24-well tissue culture plates, and were incubated at 37°C for 6h. Nonadherent proteins were detached by rinsing with PBS three times, and then 200 uL of 2% sodium dodecyl sulfate (Thermo Scientific, Rockford, IL, USA) was added to each well. Protein concentrations were determined by measuring the optical density (OD) at 570 nm on a microplate reader (Bio-Tek Instruments, Winooski, VY, USA) using Pierce Micro BCA Protein Assay kits (Thermo Scientific, Rockford, USA) in accordance with the manufacturer's instructions.

Antibacterial Assays

Bacterial Culture

S. aureus (25923; ATCC, Manassas, VA, USA) and *S. mutans* (UA159; ATCC) were used to evaluate the antibacterial properties of the nanocoatings. Both bacteria were cultured on samples in brain heart infusion broth (BHI; 37 g/L, Sigma-Aldrich, Darmstadt, Germany) in an incubator under 5% CO_2 at 37°C.

Quantitative Measurement of Bacterial Adhesion and Proliferation

The Microbial Viability Assay Kit-WST (Dojindo, Kumamoto, Japan) was used to quantitatively assess bacterial adhesion and proliferation on nanocoatings. Samples were incubated in 1 mL of bacterial suspension (10^6 cfu/mL) for 12 or 24 h. Next, the samples were gently rinsed with PBS (pH 7.4) to remove non-adherent bacteria. WST reagent with culture medium at a ratio of 1:20 (v/v) was added to each well, followed by incubation at 37°C for 2 h in darkness. Next, 100 μL of supernatant were transferred to a 96-well plate followed by measurement of the OD at 450 nm on a plate reader (Bio-Tek).

Assessment of Biofilm Formation by Crystal Violet Staining

Biofilm formation was assayed by crystal violet staining. Aliquots (1 mL) of diluted bacterial suspensions were cultured with samples at 37°C for 12 or 24 h. The samples were gently washed with PBS three times to remove planktonic bacteria. Biofilms were dried at 37°C for 1 h and stained with 200 μL of 1% (wt/vol) crystal violet (Solarbio, Beijing, China) at room temperature for 15 min. The samples were rinsed three times with PBS to remove excess stain. After drying at 37°C for 30 min, biofilm formation was quantified by solubilization of crystal violet in 95% ethanol for 15 min with agitation at 300 rpm. The crystal violet concentration was determined by measuring the OD at 570 nm on a microplate reader (Bio-Tek). The experiment was performed three times to obtain means and standard errors of the means.

Assay of Bacterial Adhesion and Biofilm Formation by Scanning Electron Microscope (SEM)

SEM was carried out to visualize the biofilms. Samples were incubated with bacterial suspensions (10^6 cfu/mL) in BHI for 12 or 24 h. The substrates were gently washed three times to remove nonadherent bacteria and fixed with 2% glutaraldehyde at 4°C overnight. After being washed in ultrapure distilled water, the biofilm samples were dehydrated by replacing the buffer with increasing concentrations of ethanol (20%, 50%, 70%, 90%, 95%, 100%, 100%, and 100%) for 15 min each. The samples were subsequently dried with a critical point dryer, sputter coated with gold, and observed using a SEM (Hitachi, Tokyo, Japan).

Cell Assays

Cell Culture

Human gingival fibroblasts (HGFs) and HaCaT immortalized human keratinocytes (ATCC) were used. HGFs were harvested from the middle third of extracted wisdom teeth or premolar roots extracted for orthodontic treatment. The study was approved by the Review Board and the Ethics Committee of Peking University Health Science Center (IRB00001052-08010) in accordance with the Declaration of Helsinki. All clinical specimens were obtained from patients who provided written informed consent to use their tissues for research purposes. They were used for experiments at passages 4–8. HaCaT cells are well characterized and standardized human keratinocytes that are readily manageable in vitro. HaCaT cells were provided by the Central Laboratory of Stomatology Hospital, Peking University. Both cells were cultured in Dulbecco's modified Eagle's medium (Gibco, Grand Island, NY, USA) containing 10% fetal bovine serum (Gibco) and 1% penicillin/streptomycin (Gibco). After reaching confluence, the cells were washed with PBS and passaged with 0.25% trypsin/ethylenediaminetetraacetic acid (Gibco). Both cell types were seeded on nano-coatings in 24-well culture plates under humidified conditions at 37°C and 5% CO_2. The medium was changed every 2–3 days.

Cell Proliferation Assay

Cell proliferation was determined using the Cell Counting Kit-8 assay (CCK-8; Dojindo, Kumamoto, Japan) according to the manufacturer's instructions. Briefly, at 1, 3, and 5 days, samples were rinsed three times with PBS, and CCK-8 reagent was added to each well with fresh culture medium at 1:10 v/v. After 2 h of incubation in darkness at 37°C, the supernatant (100 μL) from each well was added to a 96-well plate and the OD at 450 nm was read using a plate reader (Bio-Tek). All experiments were performed in triplicate.

Tumor Necrosis Factor-α (TNF-α)-Induced Inflammation and Evaluation of Anti-Inflammatory Activity

HGFs and HaCaTs were seeded on nanocoatings at 2×10^5 cells per well and incubated to approximately 80% confluence. After washing with PBS, 10 ng/L TNF-α was added; untreated cells were used as the control. Cells and supernatants were collected for mRNA and protein assays, respectively.

Quantitative Real-Time Polymerase Chain Reaction (qRT-PCR) Assay

Total RNA was extracted using TRIZOL reagent (Invitrogen, Carlsbad, CA, USA) in accordance with the manufacturer's instructions. RNA concentrations were determined spectrophotometrically at 260 nm using a NanoDrop ND-2000 spectrophotometer (Thermo Fisher Scientific, Wilmington, DE, USA). Next, RNA was used for cDNA synthesis with

a Reverse Transcription System (Toyobo, Osaka, Japan). qRT-PCR was performed using an SYBR Green Detection System with an ABI PRISM 7500 Real-Time PCR System (Applied Biosystems, Foster City, CA, USA). The amplification conditions consisted of an initial 10 min denaturation step at 95°C, followed by 40 cycles of denaturation at 95°C for 15s, annealing at 60°C for 60s, and elongation at 72°C for 30s. All reactions were carried out in triplicate. Table S1 lists the primer sequences (5′–3′); the housekeeping gene GADPH was used as an internal control. Cycle threshold (Ct) values were used to determine fold differences by the ΔΔCt method.

Enzyme-Linked Immunosorbent Assay (ELISA)

Culture supernatants were collected, centrifuged, and stored at −80°C. Interleukin-6 (IL-6) and interleukin-8 (IL-8) protein levels in supernatants were measured using ELISA kits (Meimian Industrial, Jiangsu, China) according to the manufacturer's instructions.

Statistical Analysis

All experiments were repeated at least three times. Data are reported as means ± standard deviation (SD).

Statistical analyses were performed using SPSS 20.0 software (SPSS Inc., Chicago, IL, USA). The statistical significance of differences was examined using a Student's *t* test or one-way analysis of variance combined with the Student–Newman–Keuls post hoc test. Values of $p < 0.05$ were considered significant, and $p < 0.01$ and <0.001 were considered highly and very highly significant, respectively.

Results

Surface Characterization of Plasma SiOx:H Nanocoatings

Figure 1 presents the XPS survey spectra and Table 1 lists the elemental compositions (wt%) of the samples. The O1s concentration was dominant in groups B1 and B2, and in groups A1 and A2 the plasma nanocoating C1s peaks were higher than the other peaks. The O1s peaks in B1 and B2 samples were attributed to the presence of O_2 in the mixture of TMS and O_2. The O1s peaks in B1 and B2 were comparable (55.85 and 55.34 wt%, respectively), although the deposition time of sample B2 was twice that of sample B1, implying that deposition time does not affect O1s concentration. Similarly, the percentages of C1s in A1 and A2 were 64.86 wt% and 64.88 wt%, respectively, indicating that deposition time does not affect C content. In XPS spectra, Si 2s and Si 2p peaks were observed at approximately 152 and 103 eV, respectively. The concentrations of Si2s and Si2p were almost twofold higher in samples B1 and B2

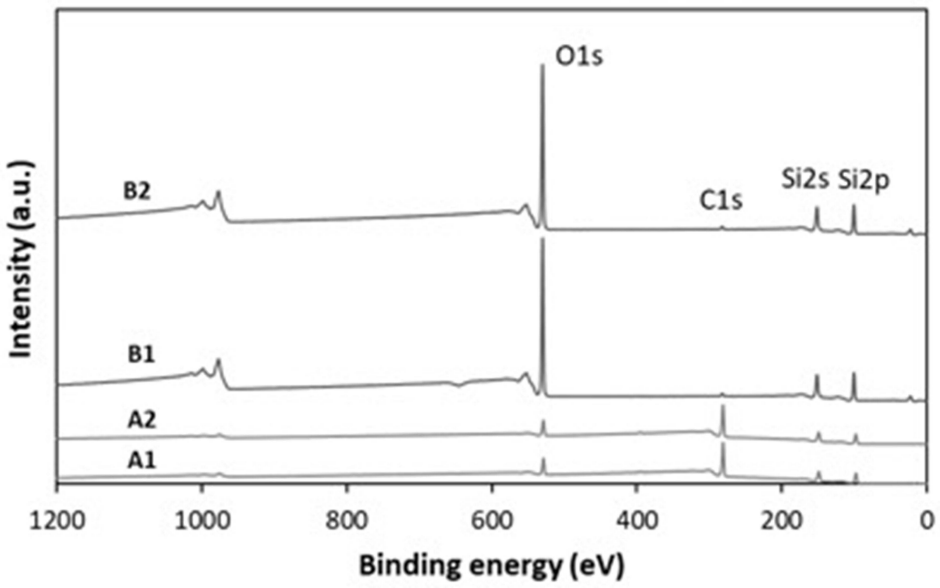

Figure 1 XPS spectra of groups A1, A2, B1, and B2.

Table 1 Surface Elemental Composition of Plasma Nanocoatings as Determined by XPS

Sample	C 1s (wt%)	O 1s (wt%)	Si 2p (wt%)
A1	64.9	8.6	26.5
A2	64.9	8.6	26.5
B1	3.4	55.9	40.8
B2	3.7	55.3-	41.0

compared to samples A1 and A2. In plasma deposition process, adding O_2 will create oxygen plasma species to etch Carbon elements by forming volatile CO or CO_2 that will be pumped out of the deposition chamber. On the other hands, oxygen plasma species will react with Si elements to deposit SiOx:H nanocoatings. As a result, the relative Si concentrations for B1 and B2 groups were higher due to the significant reduction of C content in the coatings than that for A1 and A2 groups.

Figure 2 shows AFM images that illustrated the surface morphology and surface roughness of different nanocoatings. The uncoated sample had a smooth surface morphology (Ra = 6.44 ± 1.32 nm) and group A1 and BI showed a litter rougher (Ra = 12.75 ± 1.50 nm and 11.13 ± 2.02 nm, respectively) than group A2 and B2 (Ra = 7.12 ± 0.99 nm and 6.70 ± 2.01 nm, respectively), while there was no statistical difference among the five groups.

Table 2 lists the thicknesses and water-contact angles of plasma SiOx:H nanocoatings. The plasma nanocoating thickness of groups A1, A2, B1 and B2 were 23 ± 3.1, 63 ± 5.3, 22 ± 3.9, and 60 ± 4.8 nm, respectively. Group A2 and B2 plasma nanocoatings with deposition time of 15 min and 40 min, respectively, were approximately 3-fold thicker than those of group A1 and B1, respectively. The water contact angles of groups A1 and A2 were 98° ± 1° and 101° ± 1°, and those of groups B1 and B2 were 45° ± 2° and 43° ± 1°, respectively. The water contact angle of uncoated membranes was 83° ± 2°. The water contact angle differed significantly between groups A and B ($p < 0.05$). After plasma SiOx:H nanocoating, group A became hydrophobic, whereas group B remained hydrophilic.

The amount of BSA adsorbed on plasma SiOx:H nanocoatings was decreased after 6 h incubation. Group A showed 18.63% reduction compared to the uncoated group, while group B showed 32.65% reduction nearly doubled to group A. The reduction between group A1 and A2, B1 and B2 did not show significant difference as shown in Figure 3.

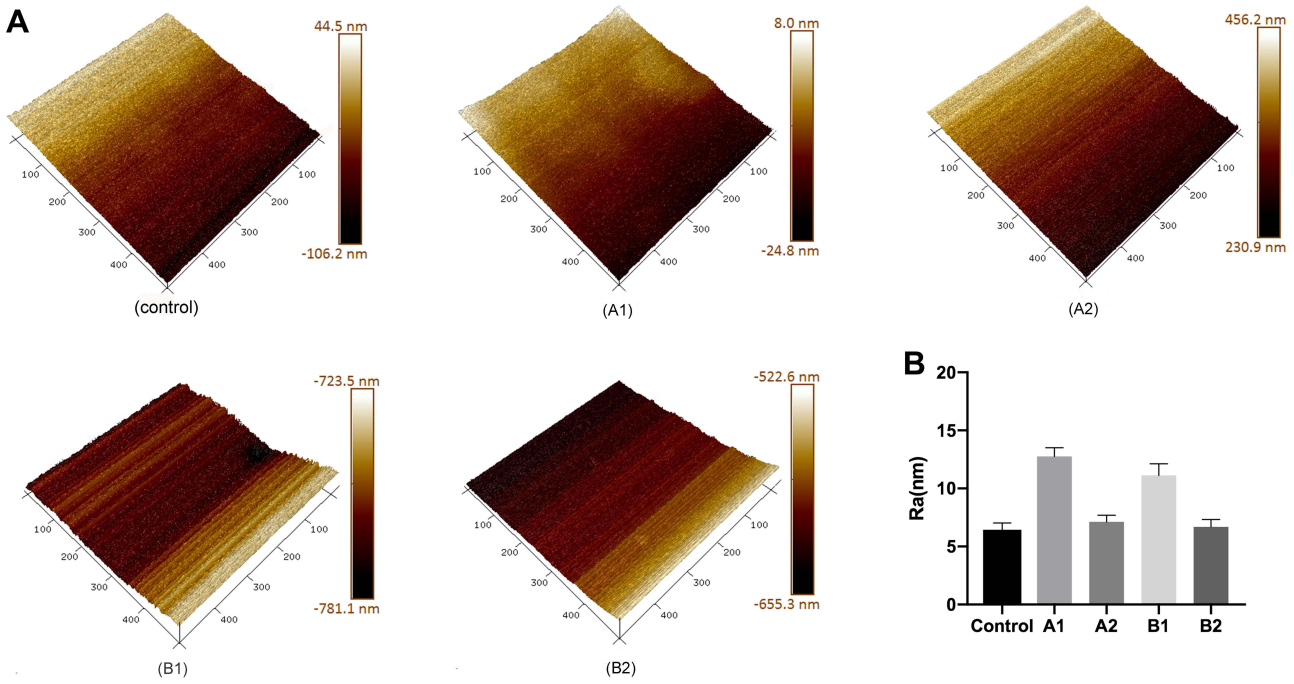

Figure 2 (**A**) Representative AFM images of nanocoatings. (**B**) The quantitative analysis of surface roughness of nanocoatings.

Table 2 Membrane Thickness and Water Contact Angle

	A1	A2	B1	B2
Thickness (nm)	23 ± 3.1	63 ± 5.3	22 ± 3.9	60 ± 4.8
Water contact angle (°)	98 ± 1	101 ± 1	45 ± 2	43 ± 1

Note: Data are means ± SD.

Abbreviations: SiOx, non-stoichiometric silicon oxides; TMS, trimethylsilane; *S. aureus, Staphylococcus aureus; S. mutans, Streptococcus mutans*; XPS, X-ray photoelectron spectrometer; AFM, atomic force microscopy; BSA, bovine serum albumin; PBS, phosphate-buffered saline; OD, optical density; BHI, brain heart infusion; SEM, scanning electron microscope; HGFs, human gingival fibroblast cells; CCK-8, cell counting kit; TNF-α, tumor necrosis factor-α; qRT-PCR, quantitative real-time polymerase chain reaction; ELISA, enzyme-linked immunosorbent assay; IL-6, interleukin-6; IL-8, interleukin-8; SD, standard deviation; COX-2, cyclooxygenase-2; MCP-1, monocytechemoattractantprotein-1.

Bacterial Adhesion and Biofilm Formation

The plasma SiOx:H nanocoatings had an antibacterial effect on *S. aureus* and *S. mutans* ($p < 0.05$) (Figure 4A and B). The numbers of viable *S. aureus* and *S. mutans* cells on the plasma SiOx:H nanocoatings were significantly lower than those on uncoated membranes. At 24 h after nanocoating, the number of viable *S. aureus* decreased by 28–75% ($p < 0.05$). The growth rate in group B was significantly lower than in group A, and the growth rate in group B2 was significantly lower than in group B1. *S. mutans* proliferation decreased by 20–50% after 12 and 24 h, respectively ($p < 0.05$). Similarly, the antibacterial effect in group B was greater than in group A, and the antibacterial effects of groups A2 and B2 were greater than those of groups A1 and B1, respectively.

Crystal violet staining was significantly decreased in the plasma SiOx:H-nanocoating groups compared to the uncoated controls (Figure 4C and D). After 24 h, groups B1 and B2 exhibited a > 60% reduction in *S. aureus* biofilm staining. The biofilm formation rates in groups A1 and A2 were 65.55% and 39.89%, respectively. *S. mutans* biofilm formation was reduced by 45–80% after 12 and 24 h, with group B2 exhibiting the greatest reduction (43%). The antibiofilm effect in group B was greater than that in group A, and the antibacterial effects of groups A2 and B2 were greater than those of groups A1 and B1, respectively.

Bacterial adhesion and biofilm formation on the nanocoatings were observed at 12 and 24 h by SEM. The plasma SiOx:H nanocoatings reduced the number of colonies (Figure 5). Multiple bacterial colonies clustered together to form biofilms (Figure 6). In untreated group, *S. mutans* formed a multilayered biofilm containing long chains of bacterial cells with numerous interstitial channels and spaces (Figure 6A). On the plasma-nanocoating group, bacterial morphology was altered and the biofilm was disrupted and discontinuous.

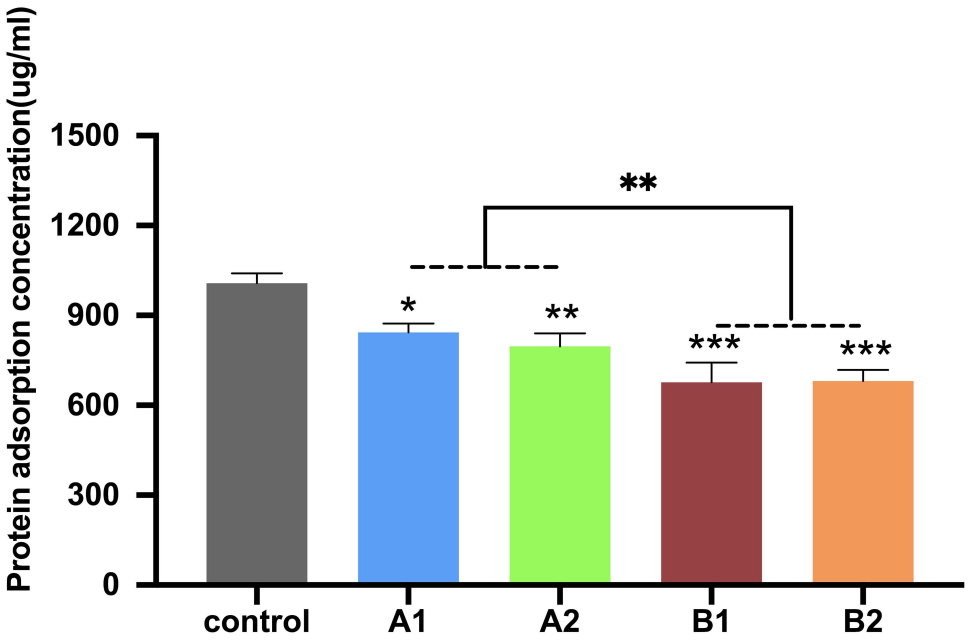

Figure 3 The average protein adsorption concentration of nanocoatings. Data are means ± SD; *$p < 0.05$, **$p < 0.01$, ***$p < 0.001$ compared to the control group.

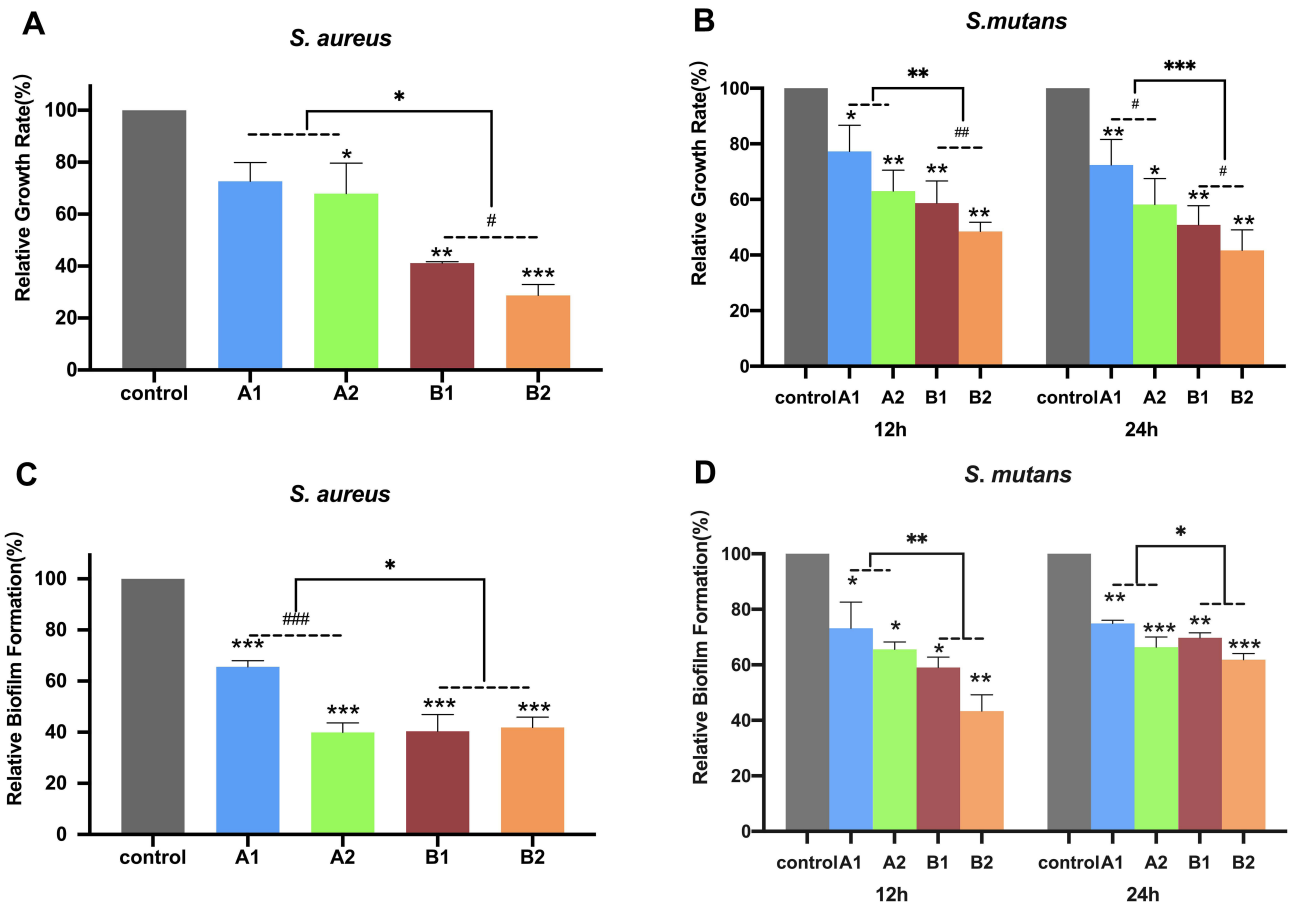

Figure 4 (**A**) Proliferation of *S. aureus* after 24 h. (**B**) Proliferation of *S. mutans* after 12 and 24 h. (**C**) *S. aureus* biofilm formation after 24 h. (**D**) *S. mutans* biofilm formation after 12 and 24 h. Data are means ± SD; $^{*}p < 0.05$, $^{**}p < 0.01$, $^{***}p < 0.001$ compared to the control group; $^{\#}p < 0.05$, $^{\#\#}p < 0.01$, $^{\#\#\#}p < 0.001$.

Plasma SiOx:H Nanocoatings Had Good Biocompatibility

Plasma SiOx:H nanocoatings did not reduce HGFs growth and promoted HaCaT growth up to 5 days (Figure 7). HGFs viability was slightly increased in group A2 on day 3 ($p < 0.05$). HaCaT proliferation in groups B1 and B2 was significantly higher than in groups A1 and A2, and in the uncoated control ($p< 0.05$).

Plasma SiOx:H Nanocoatings Downregulated the mRNA and Protein Levels of Proinflammatory Cytokines

After TNF-α stimulation, the mRNA levels of the inflammation-related cytokines IL-6 and IL-8 and the inflammatory mediator cyclooxygenase-2 (COX-2) and monocyte chemoattractant protein-1 (MCP-1) in HGFs and HaCaTs were significantly upregulated ($p < 0.05$) in the uncoated control group. The mRNA levels increased 6-fold for IL-6 and up to 33-fold for IL-8 (Figure 8). At 24 h of TNF-α stimulation, these cells had converted into an inflamed condition. In contrast, the mRNA levels of the inflammation-related cytokines in groups A1, B1, and B2 were significantly lower ($p < 0.001$). In group A2, although the MCP-1 mRNA level was downregulated, those of interler-6, IL-8, and COX-2 were higher than the control.

After TNF-α treatment, cells in the uncoated control group released more IL-6 and IL-8 than untreated cells ($p < 0.05$) (Figure 9). The IL-6 and IL-8 concentrations in groups A1, A2, B1, and B2 were lower than the uncoated control group, although some of the differences were not significant.

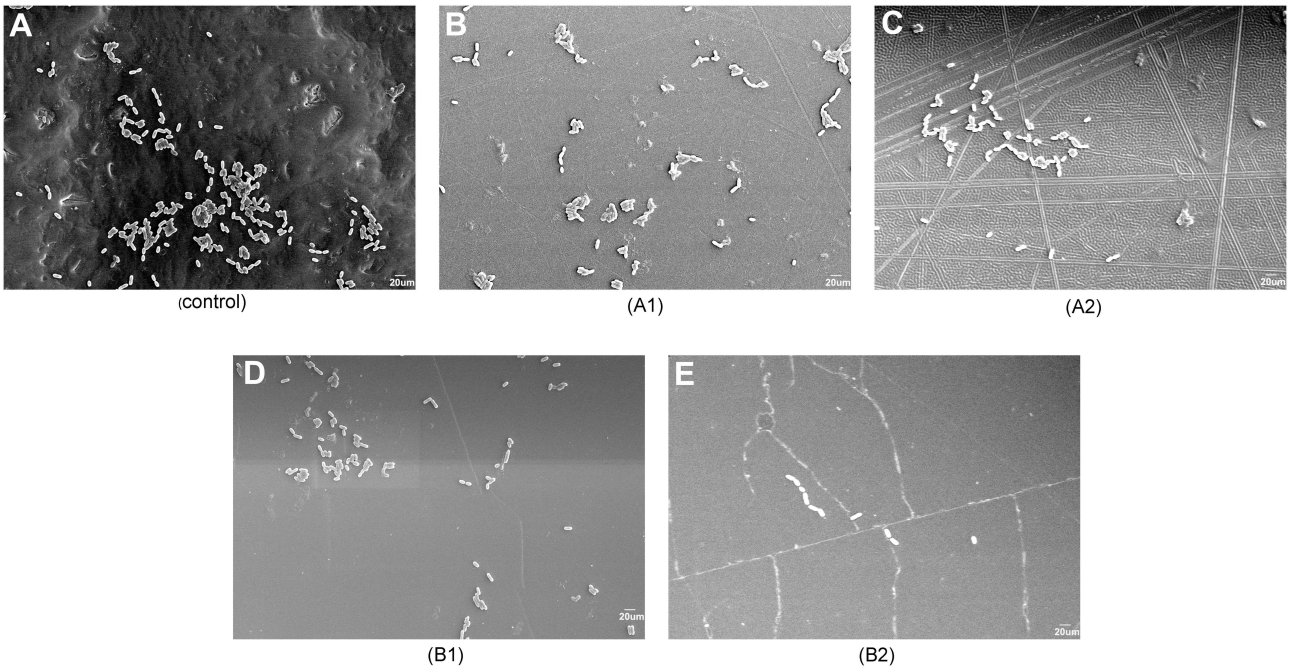

Figure 5 Representative scanning electron micrographs of *S. mutans* after 12 h of control (**A**), A1 (**B**), A2 (**C**), B1 (**D**), B2 (**E**).

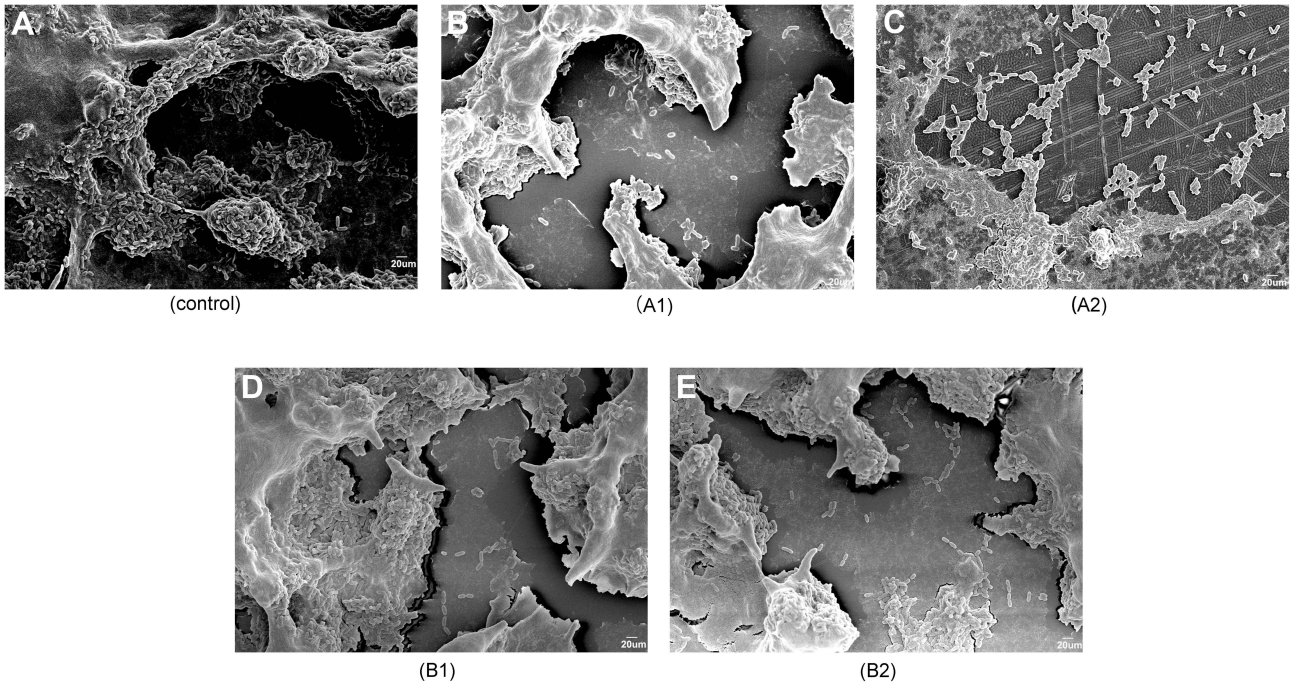

Figure 6 Representative scanning electron micrographs of *S. mutans* after 24 h control (**A**), A1 (**B**), A2 (**C**), B1 (**D**), B2 (**E**).

Discussion

Surface modification by plasma SiOx:H nanocoatings resulted in higher antibacterial activity in terms of bacterial adhesion and biofilm formation with excellent biocompatibility. Moreover, the proinflammatory cytokines and inflammatory mediator levels were decreased by the plasma SiOx:H nanocoatings, suggesting suppression of inflammatory responses without cytotoxicity, which extended the study on biological properties of the plasma SiOx:H-nanocoatings to

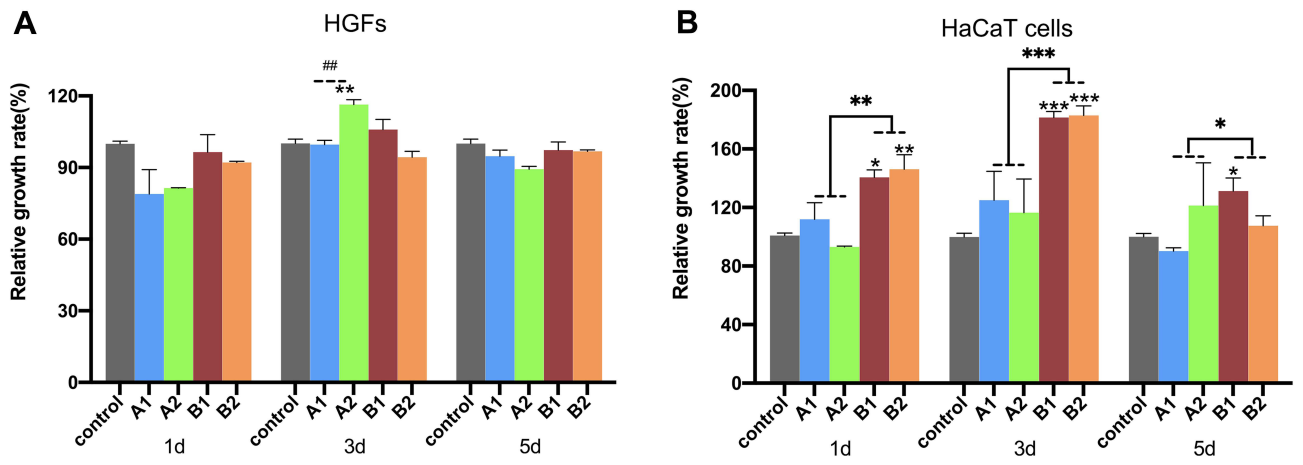

Figure 7 Proliferation of (**A**) HGFs and (**B**) HaCaTs after 1, 3, 5 days. Data are means ± SD; *$p < 0.05$, **$p < 0.01$, ***$p < 0.001$ compared to the control group; $^{\#\#}p < 0.01$.

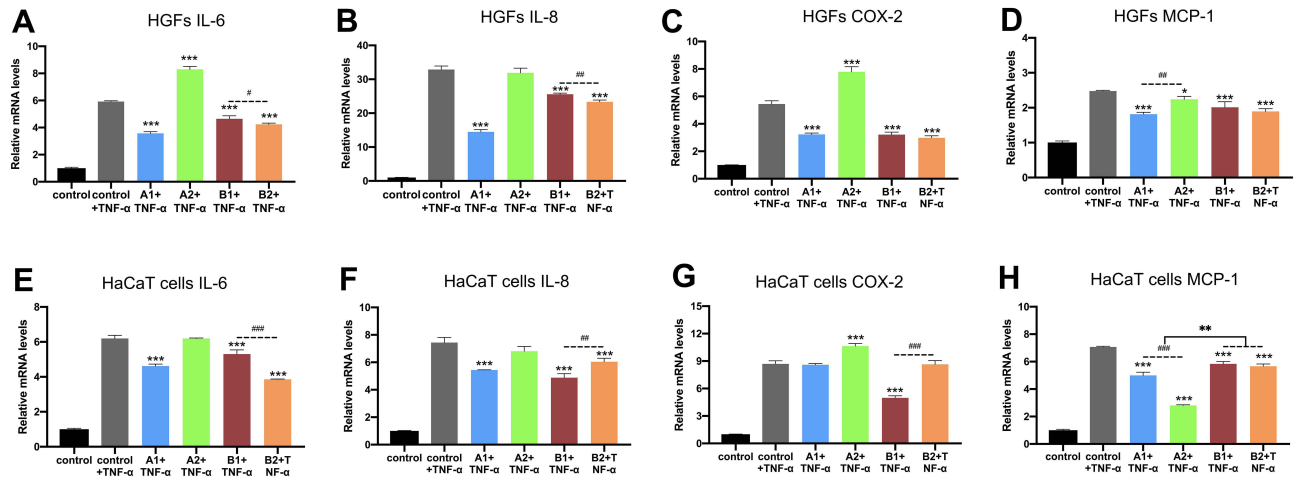

Figure 8 mRNA levels of (**A**) IL-6, (**B**) IL-8, (**C**) COX2, (**D**) MCP1 in HGFs and HaCaTs (**E**–**H**) treated with 10 ng/mL TNF-α for 24 h. Data are relative to the control group + TNF-α. *$p < 0.05$, **$p < 0.01$, ***$p < 0.001$ compared to the control group; $^{\#}p < 0.05$, $^{\#\#}p < 0.01$, $^{\#\#\#\#}p < 0.001$.

a potential anti-inflammatory activity. Therefore, plasma SiOx:H nanocoating on biomedical devices has great potential for resolving biomaterial-related infections.

To minimize risk of infection, biomaterial surfaces can be modified by various physical and chemical methods. Plasma coating is suitable for biomaterial surface modification because of its controllability and stability. Plasma nanocoating produces a stable surface by covalently bonding to the biomaterial surface.[16] In addition, the plasma nanocoating deposition conditions (gas composition, system pressure, gas flow rate, and input power) determine the material properties, including surface chemistry and wettability. Moreover, plasma nanocoating is environmentally friendly and cost-effective. Plasma nanocoating can be achieved by adjusting plasma gas compositions and plasma deposition parameters for surface modification of various biomaterials with stable surface chemistry and mechanical properties without significantly changing the topography and roughness of the substrate, thus provide good biocompatibility and wide applicability of medical biomaterials.[17] Plasma nanocoating on biomaterials with different surface chemistries have been investigated. In dentistry, plasma has been used for surface modification of various materials such as titanium, ceramics, and dentin. In this study, we used plastic dental aligner membranes as the substrate.

We successfully modulated biomaterial surface chemistry of plasma SiOx:H nanocoatings by altering the plasma gas compositions and conditions by introducing oxygen. We also controlled the plasma SiOx:H nanocoating thickness by changing the deposition time. Plasma SiOx:H nanocoatings have been applied as optical coatings, passivation layers, and

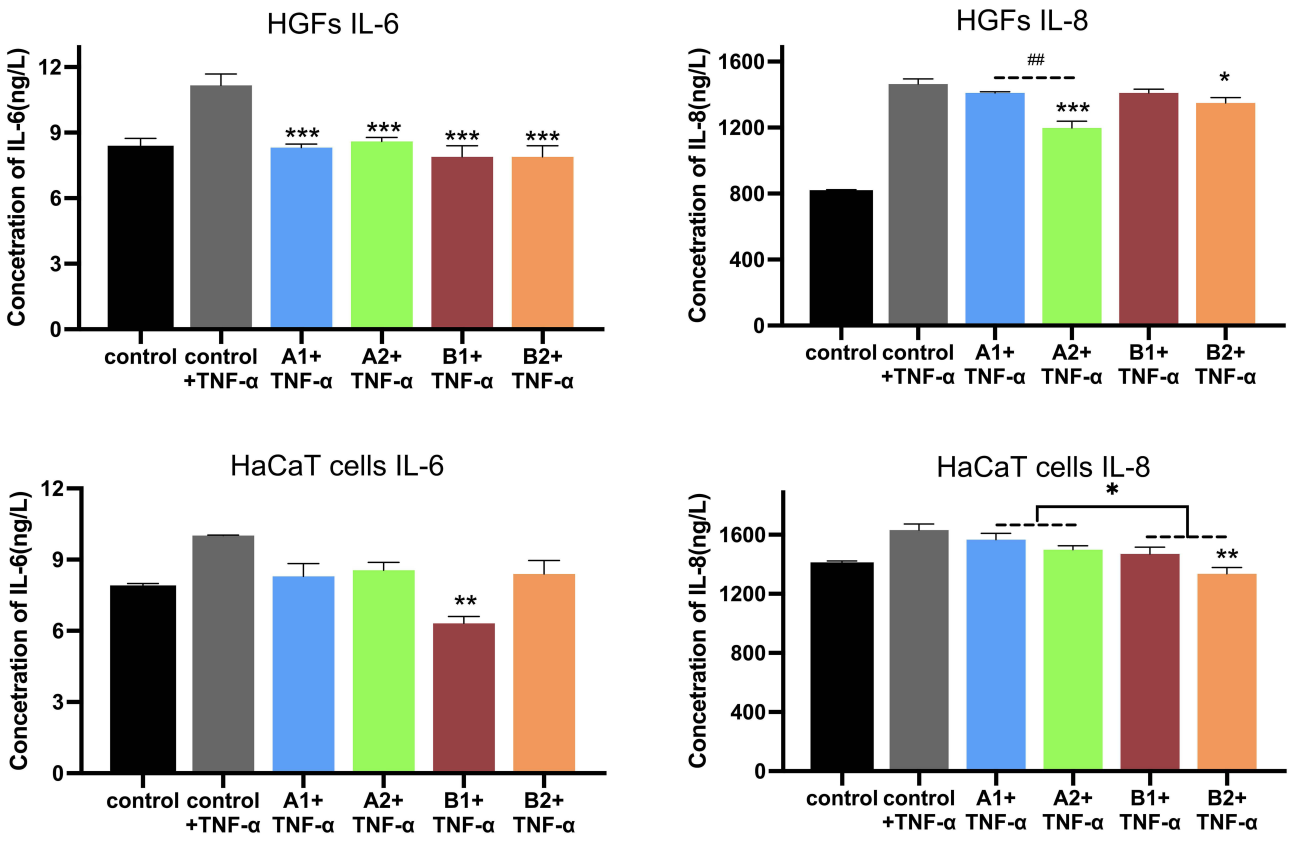

Figure 9 IL-6 and IL-8 levels in supernatant. Data are relative to the control group + TNF-α. *$p < 0.05$, **$p < 0.01$, ***$p < 0.001$ compared to the control group; ##$p < 0.01$.

interlayers in electronics because of their low dielectric constant.[18] Altering the plasma gas composition enables modulation of surface wettability. The O% and Si% concentration was dominant on the surface of group B, resulting in markedly increased hydrophobicity, and the C% concentration was dominant in group A. The Si% concentration was twofold higher in group B than in group A. The nanocoatings in groups A2 and B2 were approximately threefold thicker than those in groups A1 and B1, respectively, because of the doubled deposition time. Therefore, plasma SiOx:H nanocoating enables biomaterial surface modification by adjusting the deposition conditions.

Implant materials are substrates for bacterial adhesion and biofilm formation, which are closely related to implant infections. Therefore, reducing bacterial adhesion during the initial period following implantation is important to prevent implant-associated infection.[23] Implant-infecting bacteria are typically not sparsely distributed, single, adherent cells but form biofilms – a serious medical problem.[24] Biofilms are complex systems of microorganisms embedded within a self-produced extracellular matrix, which stabilizes the biofilm architecture and provides some resistance to environmental threats.[25] Further, chronic inflammation arises because host immune defenses and conventional antimicrobial therapies are often ineffective against biofilm bacteria.[26] The surface of biomaterials can be altered to prevent biofilm formation. In this study, the plasma SiOx:H nanocoating groups had a greater antibacterial effect on planktonic *S. aureus* and *S. mutans* and biofilms.

Interactions between biomaterial surfaces and bacteria are affected by surface hydrophobicity, roughness, topography, and chemistry.[27] The antibacterial effect was greater in group B than in group A with 30–70% reduction, and those in groups A2 and B2 were greater than those in A1 and B1, respectively. Strong anti-bacterial effects have also been reported in TMS-coated wafers that showed >98% reduction of biofilm staining, and the number of bacterial cells on TMS-coated wafers was <1% that of uncoated controls,[28] while coating the surfaces of silicone rubber with TMS and oxygen reduced biofilm formation inhibition by 90%.[21] The differences in antibacterial effects may thus be a combined result of changes in chemical compositions, surface wettability and protein adsorption. Mandracci et al reported that

silicon-oxygen thin film coatings led to a reduction of bacterial adhesion on dental composite resins.[29] Hu et al reported that functional silicon-carbon nanohybrids showed strong bacteria inhibitory effects.[30] Another study showed that increasing the ratio of oxygen enhanced inhibition of *S. aureus* biofilm formation.[22] Our results showing better antibacterial effects in group B (with higher O% and Si%) are in good agreement with these previous findings. Furthermore, the plasma SiOx:H nanocoating could improve the hydrophilicity of group B to a water contact angle of 43–45°, which could be ascribed to the higher O%. Hydrophilic biomaterials exhibit good resistance to bacterial adhesion.[31] Moreover, in our study, the plasma SiOx:H nanocoating decreased protein absorption on the surface to 67–80% compared to the uncoated group. Protein adsorption is sensitive to the underlying surface wettability, and the increasing wettability can reduce protein adsorption capacity.[32] Group B with more hydrophilic showed enhanced inhibition of protein adsorption. It also has been previously reported that the adsorption of human serum albumin or BSA is reduced on hydrophilic surfaces.[33] Biomaterials become coated with proteins from blood and interstitial fluids within nanoseconds, facilitating subsequent bacterial attachment. The interaction among proteins with bacteria plays a pivotal role in bacterial adhesion.[31] A key virulence mechanism of *S. aureus* is binding to human extracellular proteins.[25] In addition, the surface roughness of biomaterials has been recognized as another factor for surface-bacterium interactions. *Streptococcal* adhesion is sensitive to surface roughness sensitive, increasing as the roughness of composite surfaces increased from 20 nm to 150 nm.[34] In our study, all plasma SiOx:H nanocoatings had roughness levels <20 nm, below the sensitive roughness range. The improvement of antibacterial properties due to plasma SiOx:H nanocoatings was the outcome of various factors, and the specific underlying mechanisms require further investigation.

Implant infection involves complex interactions between pathogens and biomaterials, and the host immune response to both. Immune inflammatory responses are the major pathogenic mechanisms of implant infections.[4] Upon infection, pathogens and their products induce the host responses including protein adsorption, leukocyte activation and secretion of inflammatory mediators, ultimately leading to inflammation.[35] Cytokines, such as interferon-γ, and interleukin-1, IL-6, and interleukin-12, activate neutrophils and macrophages to enhance the inflammatory response and induce tissue destruction by means of activation of collagenase and other proinflammatory factors.[36] Several studies have reported increased levels of proinflammatory cytokines, such as IL-6, IL-8 and TNF- α, in patient with peri-implant diseases.[37] In this study, therefore, TNF-α was used to stimulate inflammation of HGFs and gingival epithelial cells, which are on the frontline of the immune defense system to mimic the in vivo peri-implant inflammatory microenvironment. After TNF-α stimulation for 24 h, the mRNA and protein levels of IL-6, IL-8, COX-2, and MCP-1 were significantly downregulated in the plasma nanocoating groups compared to the uncoated control group. COX-2 is the inducible isoform of cyclooxygenase, the enzyme involved in prostanoid biosynthesis, and thus induces a variety of inflammatory disorders and increases susceptibility to inflammatory diseases.[38] MCP-1 is a chemokine specific to mononuclear macrophages and stimulates inflammatory events that are important for leukocyte recruitment.[39] Reducing the levels of inflammation-related factors could alleviate the immune-inflammatory response and tissue destruction, thus preventing implant-related infection. To control the immune response, biomaterials should be capable of modulating the production of various inflammatory mediators.[15] Here, we have extended the investigation of the antibacterial properties of plasma SiOx:H nanocoatings to potential anti-inflammatory activity. Antibacterial ability and anti-inflammatory properties are sometimes contradictory. Therefore, the key point of surface modification is balancing the race between bacteria and cells.[22] To the best of our knowledge, this is the first study to show that plasma SiOx:H nanocoatings can simultaneously have antibacterial and anti-inflammatory properties.

The above improvement may be a result of the changes in protein absorption. Immediately after implantation, a biomaterial comes into contact with blood, and serum proteins adsorb to its surfaces. Therefore, the adsorption of proteins is the key determinant of cellular responses to the material surface.[27] This in turn leads to cell immune responses and the expression of proinflammatory signaling molecules. Studies have reported the successful control of protein adsorption on biomaterial surfaces to modulate immune responses by plasma polymerization.[15] In addition, polyphosphoester-coated nanocarriers reduce immune reactions by discouraging protein adsorption.[40] We speculate that reduced protein adsorption may have been responsible for the reduction in proinflammatory cytokines in the present study. However, further studies are required to characterize the cellular responses and immune reactions after plasma SiOx:H nanocoatings.

Conclusion

The results in our study indicated that plasma SiOx:H nanocoating technique could inhibit *S. aureus* and *S. mutans* adhesion and the development of biofilms, and furthermore, importantly downregulate the expression levels of inflammatory mediators after TNF-a stimulation with good biocompatibility. Moreover, plasma SiOx:H nanocoating technique could provide various chemical and physical properties by precisely adjusting deposition conditions, which offer an efficient and flexible way for surface modification of biomaterials. The specific mechanisms for these improvements will be further investigated in our future investigation. The improved antibacterial and anti-inflammatory effects demonstrated that plasma SiOx:H nanocoating technology significantly boosts the potential for resolving biomaterial-related infection. The successful application of plasma SiOx:H nanocoating technology will bring medical and financial benefits to dentistry and promote the development of biomaterials application.

Acknowledgments

This work was supported by research funds from the National Natural Science Foundation of China (Grant No. 81771119), the National Key Research and Development Program of China (Inter-Governmental International Cooperation Program, Grant No. 2019YFE0101100), the National Natural Science Foundation of China (Grant No. 82071117), the Natural Science Foundation of Beijing (Grant No. 7212136).

Disclosure

Dr Qingsong Yu has equity interest in PlasmaDent Inc, outside the submitted work. The authors declare that there are no competing interests with respect to the authorship and/or publication of this article.

References

1. Hall TJ, Villapun VM, Addison O, et al. A call for action to the biomaterial community to tackle antimicrobial resistance. *Biomater Sci*. 2020;8(18):4951–4974. doi:10.1039/d0bm01160f
2. Chaves S, Longo M, Gomez Lopez A, et al. Control of microbial biofilm formation as an approach for biomaterials synthesis. *Colloids Surf B Biointerfaces*. 2020;194:111201. doi:10.1016/j.colsurfb.2020.111201
3. Mah TF, O Toole GA. Mechanisms of biofilm resistance to antimicrobial agents. *Trends Microbiol*. 2001;9(1):34–39. doi:10.1016/S0966-842X(00)01913-2
4. Arciola CR, Campoccia D, Montanaro L. Implant infections: adhesion, biofilm formation and immune evasion. *Nat Rev Microbiol*. 2018;16(7):397–409. doi:10.1038/s41579-018-0019-y
5. Libby P. Inflammatory mechanisms: the molecular basis of inflammation and disease. *Nutr Rev*. 2007;65(12):140–146. doi:10.1301/nr.2007.dec.S140-S146
6. Harris LG, Tosatti S, Wieland M, Textor M, Richards RG. Staphylococcus aureus adhesion to titanium oxide surfaces coated with non-functionalized and peptide-functionalized poly(l-lysine)-grafted-poly(ethylene glycol) copolymers. *Biomaterials*. 2004;25(18):4135–4148. doi:10.1016/j.biomaterials.2003.11.033
7. Yougbare S, Mutalik C, Okoro G, et al. Emerging trends in nanomaterials for antibacterial applications. *Int J Nanomed*. 2021;16:5831–5867. doi:10.2147/IJN.S328767
8. Emam HE, Ahmed HB, Bechtold T. In-situ deposition of Cu 2 O micro-needles for biologically active textiles and their release properties. *Carbohydr Polym*. 2017;165:255–265. doi:10.1016/j.carbpol.2017.02.044
9. Emam HE, El-Hawary NS, Ahmed HB. Green technology for durable finishing of viscose fibers via self-formation of AuNPs. *Int J Biol Macromol*. 2017;96:697–705. doi:10.1016/j.ijbiomac.2016.12.080
10. Emam HE, Darwesh OM, Abdelhameed RM. In-growth metal organic framework/synthetic hybrids as antimicrobial fabrics and its toxicity. *Colloids Surf B Biointerfaces*. 2018;165:219–228. doi:10.1016/j.colsurfb.2018.02.028
11. Qian G, Zhang L, Liu X, et al. Silver-doped bioglass modified scaffolds: a sustained antibacterial efficacy. *Mater Sci Eng C Mater Biol Appl*. 2021;129:112425. doi:10.1016/j.msec.2021.112425
12. Yougbare S, Chang T, Tan S, et al. Antimicrobial gold nanoclusters: recent developments and future perspectives. *Int J Mol Sci*. 2019;20(12):2924. doi:10.3390/ijms20122924
13. Qian G, Zhang L, Wang G, Zhao Z, Peng S, Shuai C. 3D printed zn-doped mesoporous silica-incorporated poly-l-lactic acid scaffolds for bone repair. *Int J Bioprint*. 2021;7(2):346. doi:10.18063/ijb.v7i2.346
14. Fasolino I, Raucci MG, Soriente A, et al. Osteoinductive and anti-inflammatory properties of chitosan-based scaffolds for bone regeneration. *Mater Sci Eng C Mater Biol Appl*. 2019;105:110046. doi:10.1016/j.msec.2019.110046
15. Visalakshan RM, MacGregor MN, Sasidharan S, et al. Biomaterial surface hydrophobicity-mediated serum protein adsorption and immune responses. *ACS Appl Mater Interfaces*. 2019;11(31):27615–27627. doi:10.1021/acsami.9b09900
16. Weikart CM, Matsuzawa Y, Winterton L, Yasuda HK. Evaluation of plasma polymer-coated contact lenses by electrochemical impedance spectroscopy. *J Biomed Mater Res*. 2001;54(4):597–607. doi:10.1002/1097-4636(20010315)54:4<597::AID-JBM170>3.0.CO;2-S
17. Kim JH, Lee MA, Han GJ, et al. Plasma in dentistry: a review of basic concepts and applications in dentistry. *Acta Odontol Scand*. 2014;72(1):1–12. doi:10.3109/00016357.2013.795660

18. Choukourov A, Pihosh Y, Stelmashuk V, et al. Rf sputtering of composite SiO_x/plasma polymer films and their basic properties. *Surf Coat Technol*. 2002;151:214–217. doi:10.1016/S0257-8972(01)01622-X
19. Wang G, Shen Y, Cao Y, Yu Q, Guidoin R. Biocompatibility study of plasma-coated nitinol (NiTi alloy) stents. *IET Nanobiotechnol*. 2007;1(6):102–106. doi:10.1049/iet-nbt:20070011
20. Shen Y, Wang G, Huang X, et al. Surface wettability of plasma SiOx: hnanocoating-induced endothelial cells' migration and the associated FAK-Rho GTPases signalling pathways. *J R Soc Interface*. 2012;9(67):313–327. doi:10.1098/rsif.2011.0278
21. Xu Y, Jones JE, Yu H, et al. Nanoscale plasma coating inhibits formation of staphylococcus aureus biofilm. *Antimicrob Agents Chemother*. 2015;59(12):7308–7315. doi:10.1128/AAC.01944-15
22. Sun D, Xu D, Yang C, et al. An investigation of the antibacterial ability and cytotoxicity of a novel cu-bearing 317L stainless steel. *Sci Rep*. 2016;6:29244. doi:10.1038/srep29244
23. Khalid S, Gao A, Wang G, Chu P, Wang H. Tuning surface topographies on biomaterials to control bacterial infection. *Biomater Sci*. 2020;8(24):6840–6857. doi:10.1039/D0BM00845A
24. Hoiby N, Ciofu O, Johansen HK, et al. The clinical impact of bacterial biofilms. *Int J Oral Sci*. 2011;3(2):55–65. doi:10.4248/IJOS11026
25. Paharik AE, Horswill AR, Kudva IT, Nicholson TL. The staphylococcal biofilm: adhesins, regulation, and host response. *Microbiol Spectr*. 2016;4(2):1–48. doi:10.1128/microbiolspec.VMBF-0022-2015
26. Su L, Li Y, Liu Y, An Y, Shi L. Recent advances and future prospects on adaptive biomaterials for antimicrobial applications. *Macromol Biosci*. 2019;19(12):e1900289. doi:10.1002/mabi.201900289
27. Cameron JW, Richard EC, David IL, Mark JP. Mediation of biomaterial-cell interactions by adsorbed proteins: a review. *Tissue Eng*. 2005;11(1–2):1–18. doi:10.1089/ten.2005.11.1
28. Ma Y, Chen M, Jones JE, et al. Inhibition of staphylococcus epidermidis biofilm by trimethylsilane plasma coating. *Antimicrob Agents Chemother*. 2012;56(11):5923–5937. doi:10.1128/AAC.01739-12
29. Mandracci P, Mussano F, Ceruti P, et al. Reduction of bacterial adhesion on dental composite resins by silicon-oxygen thin film coatings. *Biomed Mater*. 2015;10(1):015017. doi:10.1088/1748-6041/10/1/015017
30. Hu G, Song B, Jiang A, et al. Multifunctional silicon-carbon nanohybrids simultaneously featuring bright fluorescence, high antibacterial and wound healing activity. *Small*. 2019;15(9):e1803200. doi:10.1002/smll.201803200
31. Song F, Koo H, Ren D. Effects of material properties on bacterial adhesion and biofilm formation. *J Dent Res*. 2015;94(8):1027–1034. doi:10.1177/0022034515587690
32. Spriano S, Sarath Chandra V, Cochis A, et al. How do wettability, zeta potential and hydroxylation degree affect the biological response of biomaterials? *Mater Sci Eng C Mater Biol Appl*. 2017;74:542–555. doi:10.1016/j.msec.2016.12.107
33. Jeyachandran YL, Mielczarski E, Rai B, Mielczarski JA. Quantitative and qualitative evaluation of adsorption/desorption of bovine serum albumin on hydrophilic and hydrophobic surfaces. *Langmuir*. 2009;25(19):11614–11620. doi:10.1021/la901453a
34. Mei L, Busscher HJ, Van der mei HC, Ren Y. Influence of surface roughness on streptococcal adhesion forces to composite resins. *Dent Mater*. 2011;27:770–778. doi:10.1016/j.dental.2011.03.017
35. Zhou G, Groth T. Host responses to biomaterials and anti-inflammatory design-a brief review. *Macromol Biosci*. 2018;18(8):e1800112. doi:10.1002/mabi.201800112
36. Seymour GJ, Gemmell E. Cytokines in periodontal disease: where to from here? *Acta Odontol Scand*. 2001;59(3):167–173. doi:10.1080/000163501750266765
37. Renvert S, Widen C, Persson GR. Cytokine expression in peri-implant crevicular fluid in relation to bacterial presence. *J Clin Periodontol*. 2015;42(7):697–702. doi:10.1111/jcpe.12422
38. Schaefer AS, Richter GM, Nothnagel M, et al. COX-2 Is associated with periodontitis in Europeans. *J Dent Res*. 2010;89(4):384–388. doi:10.1177/0022034509359575
39. Singh PK, Parsek MR, Greenberg EP, et al. A component of innate immunity prevents bacterial biofilm development. *Nature*. 2002;417(6888):552–555. doi:10.1038/417552a
40. Simon J, Wolf T, Klein K, Landfester K, Wurm FR, Mailander V. Hydrophilicity regulates the stealth properties of polyphosphoester-coated nanocarriers. *Angew Chem Int Ed Engl*. 2018;57(19):5548–5553. doi:10.1002/anie.201800272